Reconfigurable transmitarrays at Ka-Band with beam-forming and polarization agility

Antonio Clemente, Reda Madi, Francesco Foglia Manzillo, Maciej Smierzchalski, Jacques Reverdy, Ronan Sauleau

Reconfigurable Transmitarrays at Ka-Band with Beam-Forming and Polarization Agility

Antonio Clemente[1], Reda Madi[1], Francesco Foglia Manzillo[1], Maciej Smierzchalski[1], Jacques Reverdy[1], Ronan Sauleau[2]

[1] CEA-Leti, Université Grenobe Alpes, F-38000 Grenoble, France, antonio.clemente@cea.fr

[2] Univ Rennes, CNRS, IETR (Institut d'Electronique et des Technologies du numéRique) - UMR CNRS 6164, F-35000 Rennes, France

***Abstract*—This paper presents transmitarray-based antenna solutions for SATCOM transmit (*Tx*) user terminals at Ka-band. We propose a new electronically-reconfigurable unit-cell structure which combines a 2-bit phase control with circular polarization agility. Six p-i-n diodes are integrated into the proposed unit-cell implemented by stacking two half-wavelength periodic structures: a reconfigurable phase-shift module and a switchable linear-to-circular polarization converter. The two structures, developed on a standard PCB stack-up, are separated by an optimized air gap. A 576-element square transmitarray with 3456 integrated p-i-n diodes has been designed, optimized, and fabricated. To enhance the advantages of this innovative architecture, its performance is compared to the one of our previous transmitarray demonstration based on a random sequential combination of 576 vertically- and horizontally-polarized 2-bit reconfigurable unit-cells. To the best of our knowledge, this represents the first demonstration of transmitarray with two stacked reconfigurable functionalities.**

***Index Terms*—transmitarray antennas, SATCOM, beam-forming, electronic beam-scanning, electronic polarization control, linear-to-circular poalrization converter, wide scanning, T-RIS.**

I. Introduction

The 2019 GMSA report on the state of internet mobile connectivity estimated that 40% of Earth's regions were without adequate network coverage [1]. This corresponds to around 4 billion people on the planet without broadband Internet access. Furthermore, the COVID-19 pandemic has highlighted the need for an efficient global connection to support advanced and essential services such as remote health, home working, or online learning. In this context, Low-Earth Orbit (LEO) satellite technologies could be a solution to reduce the digital divide between urban and rural areas, and developed and least-developed countries. Thanks to a finely-meshed network of several thousands of satellites, this innovative network paradigm could provide high-speed internet connectivity everywhere on the globe [2],[3].

User terminal antennas for SATCOM-on-the-move (SOTM) require innovative technologies to fit with the strict applicative requirements, in terms of radioelectrical performances, mobility, integration constraints, and cost. These requirements become extremely challenging at K/Ka-band, where the antenna should operate in full-duplex and dual circular-switchable polarization. Orthogonal polarization is required between up-link (*Tx*, 27.5-31.0 GHz) and down-link (*Rx*, 17.3-21.2 GHz) frequency ranges to improve the *Tx*/*Rx* isolation. Furthermore, electronically beam-scanning over a wide field of view is required to guarantee the continuity of the link, because of the ultra-directive beam resulting from the EIRP and G/T specifications. Phased-array antennas with integrated circuits (IC) are very flexible architectures to electronically steer the radiated beam [4],[5]. However, the development costs of the ICs, the intrinsic power consumption, the periodic calibration constraints of the radiofrequency chains, and the scalability limitations restrict the massive deployment of these technologies.

An alternative and very promising solution for SOTM applications is based on spatially-fed antenna systems such as reflectarrays [6]-[8] and transmitarrays [9]-[18]. The use of spatial illumination reduces the power distribution loss when a large aperture is required. Furthermore, in the case of transmitarrays, a flat panel composed of several hundreds or thousands of unit-cells can be implemented by considering near-field illumination techniques [9]. Varactors [9]-[11], RF-MEMS switches [12], or p-i-n diodes [13]-[19] can be integrated into the radiating aperture to electronically control the transmission phase of the unit-cells, dynamically steer/shape the antenna beam, and manipulate the polarization of the impinging or transmitting electromagnetic waves.

This contribution proposes a new transmitarray architecture capable to generate electronic beam-scanning and circular polarization control, when limiting the implementation and phase-quantization losses compared to previous solutions [13]-[16],[18]. Sequential rotation schemes with 1-bit of phase resolution for beam-steering are typically used in the literature [15],[16]. Inspired by our pioneering work [16], we recently demonstrated the possibility to mitigate the quantization loss and improve the antenna gain by around 2.5 dB [18]. The idea was to randomly combine vertical- (V) and horizontal-polarized (H) unit-cells with a phase resolution of 2 bits. Despite the gain improvement, 3 dB of losses were achieved still due to the fact that the circular polarization is obtained by combining two orthogonal linear polarizations. In this paper, to drastically reduce the polarization loss, the 2-bit unit-cell has

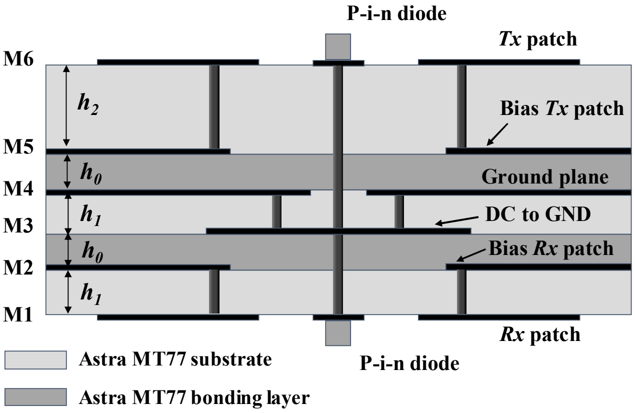

(a)

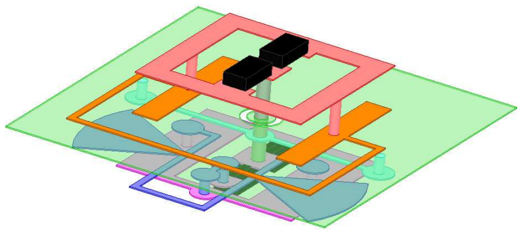

(b)

Fig. 2. 2-bit linearly-polarized unit-cell with p-i-n diodes. (a) Dielectric stack-up and (b) 3D view

been opportunely combined for the first time with a reconfigurable linear-to-circular polarization converter.

II. P-i-n Diode Based Unit-Cell for Phase-Shift and Polarization Control

This section details the building blocks of the electronically-reconfigurable unit-cell with independent control on the transmission phase and circular polarization. This structure combines, in an optimized way, the 2-bit reconfigurable unit-cell demonstrated in [17],[18] and the switchable polarizer briefly introduced in our preliminary work [20]. Finally, the performance of the complete structure are presented in the last subsection.

A. 2-bit Linearly-Polarized Unit-Cell

First, the 2-bit unit-cell architecture is shortly reintroduced here. Note that further details can be found in our previous works [17],[18]. Three Isola Atra MT77 dielectric substrates and two bonding films are opportunely stacked to achieve a total thickness, including the six metal layers M1-M6, of around 1.23 mm (Fig. 1(a)). The unit-cell period is equal to 5.1 mm along the two directions. It combines a 1-bit and a 90° phase-shift radiating element printed on the top and bottom layers, respectively. The 3D schematic view of this unit-cell is presented in Fig. 1(b). To obtain the 2-bit transmission phase resolution, two p-i-n diodes are integrated on both the top (M6) and bottom (M1) metal layers. They are controlled by considering the two bias lines integrated on the inner layers M2 and M5. A ground

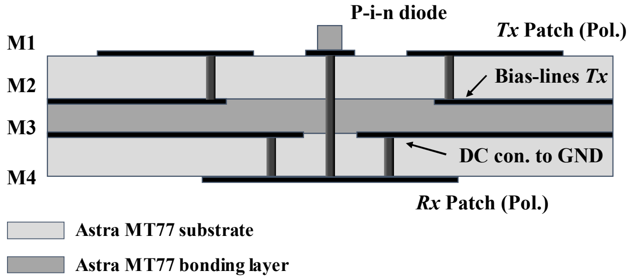

(a)

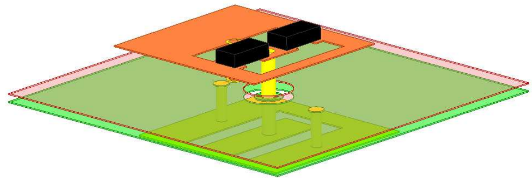

(b)

Fig. 1. Linear to circular polarization converter with p-i-n diodes. (a) Dielectric stack-up and (b) 3D view.

plane and a DC connection are realized on the layers M3 and M4.

The unit-cell has been designed and optimized in a periodic boundary condition environment using the commercial software Ansys Electronics v2020. Under normal incidence, the transmission losses are lower than 2 dB in the frequency band 28.0-31.5 GHz. Furthermore, four phase states with a relative phase-shift of 90°±15° are obtained by opportunely switching the four p-i-n diodes from the *on* to the *off* states [17].

B. Switchable Linear-to-Circular Polarization Converter

The switchable linear-to-circular polarization converter has been introduced in our preliminary paper [20]. Its constitutive unit-cell has the same aperture size as the 2-bit unit-cell, namely 5.1×5.1 mm^2. The selected dielectric stack-up is represented in Fig. 2(a). It consists of two identical substrates Isola Astra MT77, a bonding film, and four metal layers (M1-M4). The 3D schematic view of the proposed element is depicted in Fig. 2(b). The receiving metal layer (M4) includes a linearly-polarized square patch loaded by a U-shaped slot. At the transmitting layer (M1), an active patch loaded by an asymmetric O-shaped slot and two p-i-n diodes are used. In contrast to [19], where a truncated-corner patch was used, asymmetric excitation is selected here to generate a switchable circular polarization. The two patches are connected with a metallized via placed at the center of the unit-cell. A ground plane with a central hole and the bias line are realized on the inner layers. Metalized vias are used to connect the two patch antennas to the ground plane and the bias line, respectively. An impinging linearly-polarized electromagnetic wave on the receiving layer is than converter in a circularly-polarized wave in the transmission layer. By switching the two p-i-n diodes between the *on* and the *off* bias states, circular-polarization manipulation is demonstrated [20].

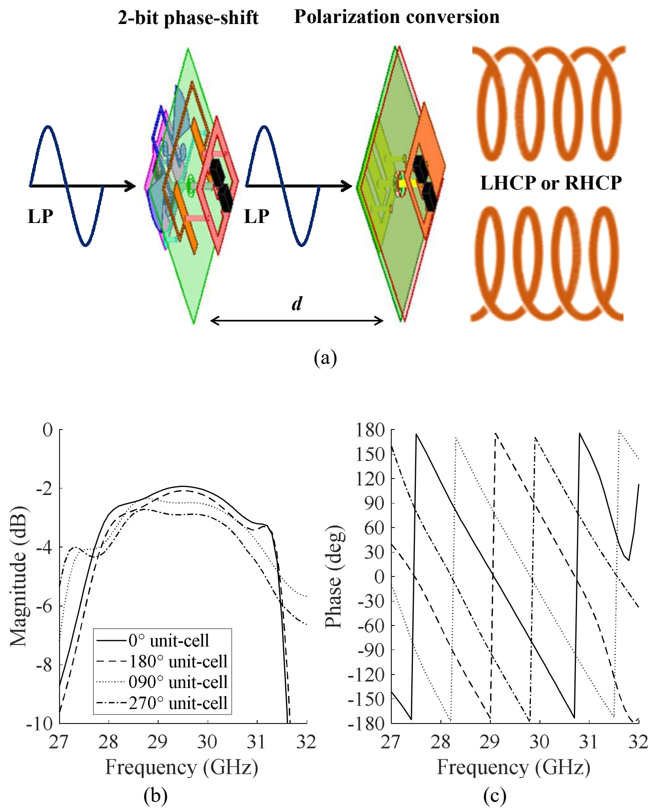

Fig. 3. Combination of the 2-bit unit-cell and linear-to-circular polarization converter. (a) Schematic view and simulated transmission coefficient for the LHCP: (b) magnitude and (c) phase.

As in the case of the 2-bit unit-cell, also this element has been designed and optimized in full-wave using periodic boundary conditions. A wideband behavior of 15.2 and 11.4% has been achieved with a minimum insertion loss of 0.70 and 0.55 dB for the two polarization states, namely LHCP and RHCP, respectively.

C. *Phase-Shift and Polarization Control*

The two unit-cell structures described in the previous sections are opportunely combined to implement both phase-shift and circular polarization electronic control. The 3D schematic view of this new unit-cell is presented in Fig. 3(a). A specific cascade equivalent model of the different layer has been developed to optimize the air gap (*d*) between the two structures, which has been found equal to around a quarter of wavelength to maximize the transmission coefficient (Fig. 3(b)). The presentation of the equivalent model and its validation by full-wave simulations is out of the scope of this paper.

The optimized structure has been simulated in a periodic boundary condition full-wave environment. The magnitude and phase of the transmission coefficients achieved for the LHCP and for the selected 2-bit phase resolution are presented in Fig. 3(b) and (c), respectively. As expected, at the best configuration the total insertion loss results as the combination of the losses of the two structures. A wideband behavior is achieved in both LHCP and RHCP configurations.

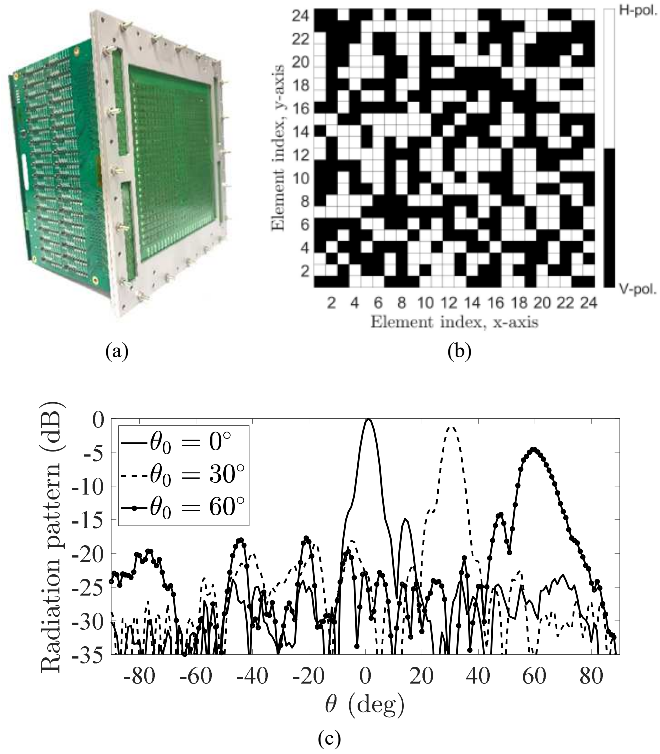

Fig. 4. Prototype I: (a) photograph, (b) random arrangement of V- and H-polarized unit-cells, and (c) measured radiation patterns of several RHCP beams on the E-plane.

III. Electronically-Steerable Transmitarrays at Ka-band

In this section, two transmitarrays are analyzed. They are based on the two unit-cell architectures presented in Section III: (1) 2-bit unit-cell, and (2) stacked 2-bit/polarization converter unit-cell. Both transmitarrays are illuminated by a 10-dBi standard gain horn (focal distance 70 mm) and have been fabricated.

A. *Prototype I: Random Combination of V and H Linearly-Polarized Unit-Cells*

The 2-bit unit-cell has been used to implement a 24×24-element transmitarray (Fig. 4(a), named prototype I)). 2304 p-i-n diodes have been integrated on the antenna aperture. In order to achieve both electronic beam-scanning and circular polarization switching, a random combination of V- and H-polarized unit-cells has been selected on the transmitting layer of the radiating aperture (Fig. 4(b)). This distribution has been optimized to minimize the axial ratio value (0.1 and 0.7 dB at 30.25 GHz for the RHCP and LHCP, respectively.

The fabricated prototype includes an *ad-hoc* steering logic, designed to minimize the power consumption of the whole beam-former system (< 15 W, including a µ-controller). Note that for the full SACTOM antenna system, the power consumption of the associated power amplifier should be included.

The antenna system has been characterized at the CEA-Leti anechoic chamber. The measured radiation patterns for a selection of 30.25-GHz-beams are presented in Fig. 4(c). As per simulations, the peak broadside gain is 25.5 dB at 30.75 GHz, corresponding to an aperture efficiency of 18.0%. This efficiency is about twice that attained by dual-circular polarized transmitarray presented in [16]. In agreement with the unit-cell radiation pattern, the scan loss is equal to 1 dB at 30° and 4.6 dB at 62°.

B. Prototype II: Linearly-Polarized Transmitarray with Stacked Linear to Circular Polarization Converter

To validate the proposed stacked 2-bit/polarization converter unit-cell, a square transmitarray with 24×24 elements has been designed (named prototype II). The antenna layout has been optimized considering an *ad-hoc* numerical tool based on ray tracing and full-wave simulations. The antenna is composed of a 2-bit linearly-polarized aperture and a reconfigurable stacked polarizer. The photograph of the realized prototype is presented in Fig. 5(a). The antenna includes 2034 and 1152 p-i-n diodes, respectively, on the linearly-polarized aperture and on the polarizer layer.

The simulated peak gain over the frequency band 28-32 GHz has been plotted in Fig. 5(b). A gain of 26.9 dBi has been achieved at 30.75 GHz, demonstrating a 1.4 dB of gain improvement if compared to the results achieved with the prototype I. The corresponding aperture efficiency of the prototype II is equal to 24.8%.

To complete our analysis the peak gain achieved in simulation by considering only the 2-bit linearly-polarized aperture (LP TA) has been plotted in Fig. 5(b). From the picture, it is clear that a gain improvement of 3 dB (aperture efficiency of 35.8%) is achieved if compared to prototype I. This explains clearly the polarization loss in the prototype I due to the combination of V- and H-polarized unit-cells.

IV. Conclusion

This paper presents new results of our research activity on reconfigurable transmitarrays for SATCOM applications at Ka-band. The SOTM specifications impose the need for high gain, wide beam-scanning, and circular polarization switching. To this purpose, two unit-cell architectures with a 2-bit phase resolution have been presented. The first unit-cell operates in linear polarization. The second architecture combines the linearly-polarized unit-cell with a reconfigurable linear-to-circular polarization converter. P-i-n diodes have been used to control the transmission phase and the polarization switching functions.

Two transmitarray prototypes integrating 2304 and 3456 have been designed and fabricated. The use of the unit-cell with the polarization converter allows the improvement of the aperture efficiency from 18.0% to 24.8%, if compared to the prototype where the polarization switching is implemented by the combination of V- and H-polarized unit-cells.

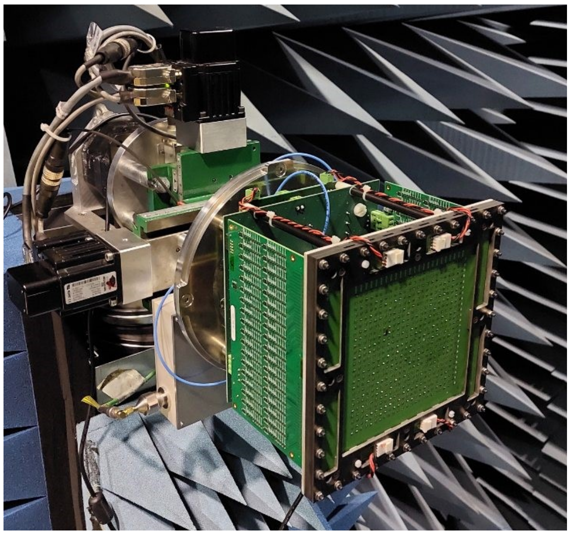

(a)

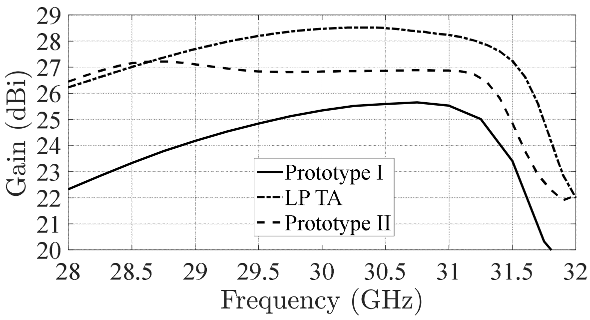

(b)

Fig. 5. Prototype II: (a) photograph. (b) Simulated peak gain, including comparison with the performance achieved with the prototype I and the 2-bit linearly-polarized transmitarray.

Acknowledgment

This work was partly supported by the National Research Agency (ANR) through the project ANR-ASTRID ArtiKa under grant ANR-20-ASTR-0014-01, and H2020 project RISE-6G.

References

[1] K. Bahia and S. Suadi, “The state of mobile internet connectivity report 2019,” GSMA, London, U.K., 2019.

[2] R. Correia, T. Varum, J. N. Matos, A. Oliveira, and N. Borges Carvalho, “User terminal segments for low-Earth orbit satellite constellations,” *IEEE Microwave Mag.*, vo. 23, no. 10, pp. 47-58, Oct. 2022.

[3] I. del Portillo, B.G. Cameron, and E. F. Crawley, “A technical comparison of three low earth satellite constellation systems,” *Acta Astronautica*, vol. 159, pp. 123-135, Jun. 2019.

[4] K. K. Wei Low, S. Zihir, T. Kanar, and G. M. Rebeiz, “A 27-31-GHz 1024-element Ka-band SATCOM phased-array transmitter with 49.5-dBW peak EIRP, 1-dB AR, and ±70° beam scanning,” *IEEE Trans. Microwave Theory Techn.*, vol. 70, no. 3, pp. 1757-1768, Mar. 2022.

[5] X. Luo, et al., “A scalable Ka-band 1024-element transmit dual-circularly-polarized planar phased array for SATCOM applications,” *IEEE Access*, vol. 8, pp. 156084 – 156095, 2020.

[6] J.-M. Baracco, P. Ratajczak, P. Brachat, J.-M. Fargeas, and G. Toso, "Ka-based reconfigurable reflectarrays using varactor technology for space applications: a proposed design," *IEEE Antennas Propag. Mag.*, vol. 64, no. 1, pp. 27-38, Dec. 2021.

[7] H. Yang et al., "A 1600-element dual-frequency electronically reconfigurable reflectarray at X/Ku bands," *IEEE Trans. Antennas Propag.*, vol. 65, no. 6, pp. 3024–3032, Jun. 2017.

[8] J.-B. Gros, V. Popov, M. Odit, and G. Lerosay, "A wave physics approach to electronically steerable antennas," in *Proc. 35th Annual Small Satellite Conf.*, Logan, Utah, USA, 7-12 Aug. 2021.

[9] G. Nicholls and S. V. Hum, "Full-space electronic beam-steering transmitarray with integrated leaky-wave feed," *IEEE Trans. Antennas Propag.*, vol. 64, no. 8, pp. 3410–3422, Aug. 2016.

[10] J. R. Reis, R. F. S. Caldeirinha, A. Hammoudeh, and N. Copner, "Electronically reconfigurable FSS-inspired transmitarray for 2-D beamsteering," *IEEE Trans. Antennas Propag.*, vol. 65, no. 9, pp. 4880–4885, Sep. 2017.

[11] M. Frank, F. Lurz, R.Weigel, and A. Koelpin, "Electronically reconfigurable 6 × 6 element transmitarray at K-band based on unit cells with continuous phase range", *IEEE Antennas Wireless Propag. Lett.*, vol. 18, no. 4, pp. 796–800, Apr. 2019.

[12] C.-C. Cheng, B. Lakshminarayanan, and A. Abbaspour-Tamijani, "A programmable lens-array antenna with monolithically integrated MEMS switches," *IEEE Trans. Microw. Theory Techn.*, vol. 57, no. 8, pp. 1874–1884, Aug. 2009.

[13] C. Huang, W. Pan, X. Ma, B. Zhao, J. Cui, and X. Luo, "Using reconfigurable transmitarray to achieve beam-steering and polarization manipulation applications," *IEEE Trans. Antennas Propag.*, vol. 63, no. 11, pp. 4801–4810, Nov. 2015.

[14] Y. Wang, S. Xu, F. Yang and D. H. Werner, "1 bit dual-linear polarized reconfigurable transmitarray antenna using asymmetric dipole elements with parasitic bypass dipoles," *IEEE Trans. Antennas Propag.,* vol. 69, no. 2, pp. 1188-1192, Feb. 2021.

[15] C.-W. Luo, G. Zhao, Y.-C. Jiao, G.T. Chen, and Y.-D. Yan, "Wideband 1 bit reconfigurable transmitarray antenna based on polarization rotation element," *IEEE Antennas Wireless Propag. Lett.*, vol. 20, no. 5, pp. 798–802, May 2021.

[16] L. Di Palma, A. Clemente, L. Dussopt, R. Sauleau, P. Potier, and P. Pouliguen, "Circularly-polarized reconfigurable transmitarray in Ka-band with beam scanning and polarization switching capabilities," *IEEE Trans. Antennas Propag.*, vol. 65, no. 2, pp. 529-540, Feb. 2017.

[17] A. Clemente, F. Diaby, L. Di Palma, L. Dussopt, and R. Sauleau, "Experimental validation of a 2-bit reconfigurable unit-cell for transmitarrays at Ka-band," *IEEE Access*, vol. 8, pp. 114991-114997, 2020.

[18] F. Foglia Manzillo, M. Smierzchalski, J. Reverdy, and A. Clemente, "A Ka-band beam-steering transmitarray achieving dual-circular polarization," in *Proc. 15th Eu. Conf. Antennas Propag.* (*EuCAP 2021*), Dusseldorf, Germany, 22-26 Mar. 2021.

[19] L. Di Palma, A. Clemente, L. Dussopt, R. Sauleau, P. Potier, and P. Pouliguen, "Experimental characterization of a circularly-polarized 1-bit unit-cell for beam steerable transmitarrays at Ka-band," *IEEE Trans. Antennas Propag.*, vol. 67, no. 2, pp. 1300-1305, Feb. 2019.

[20] R. Madi, A. Clemente, and R. Sauleau, "A switchable linear to circular polarization converter using PIN diodes," in *Proc. Int. Symp. Antennas Propag.* (*ISAP 2021*), Taipei, Taiwan, 19-22 Oct. 2021.